

## Global magnetospheric-ionospheric oscillations initiated by a solar wind pressure impulse

Chao-Song Huang,<sup>1</sup> J. C. Foster,<sup>1</sup> G. D. Reeves,<sup>2</sup> J. Watermann,<sup>3</sup> J. H. Sastri,<sup>4</sup> K. Yumoto,<sup>5</sup> and P. Song<sup>6</sup>

Received 1 May 2002; revised 6 March 2003; accepted 4 April 2003; published 10 June 2003.

[1] We present simultaneous observations of long-period ( $\sim 1$  hour) global magnetospheric-ionospheric oscillations with multiple spacecraft and ground-based instruments. These oscillations occurred following a major increase in the solar wind dynamic pressure. When the solar wind pressure impulse impinged on the magnetosphere, oscillations of energetic plasma particles in the ring current region were excited. The strongest oscillations came from electrons in the energy range of 75–225 keV with periods of 55–80 min. Ground magnetometers measured periodic ( $\sim 1$  hour) enhancements of ionospheric currents from the auroral to equatorial latitudes. However, the solar wind pressure and IMF in this event did not show variations similar to the energetic particle oscillations and/or ground magnetometer deviations. We suggest that the magnetosphere has an intrinsic period of  $\sim 1$  hour during quiet times. The magnetospheric oscillations with this period can be initiated by a solar wind pressure impulse. After the initiation the solar wind no longer plays a role in the subsequent evolution of the magnetospheric oscillations. **INDEX TERMS:** 2736 Magnetospheric Physics: Magnetosphere/ionosphere interactions; 2784 Magnetospheric Physics: Solar wind/magnetosphere interactions; 2778 Magnetospheric Physics: Ring current; 2435 Ionosphere: Ionospheric disturbances; **KEYWORDS:** oscillations, magnetospheric oscillations, long periods, ring current, drift echoes

**Citation:** Huang, C.-S., J. C. Foster, G. D. Reeves, J. Watermann, J. H. Sastri, K. Yumoto, and P. Song, Global magnetospheric-ionospheric oscillations initiated by a solar wind pressure impulse, *J. Geophys. Res.*, 108(A6), 1232, doi:10.1029/2002JA009465, 2003.

### 1. Introduction

[2] In recent years, long-period (tens of minutes) perturbations have been observed in the magnetosphere and ionosphere. Rinnert [1996] found quasiperiodic (40–60 min) enhancements of electron density in the auroral *E* region. Lessard *et al.* [1999] observed periodic ( $\sim 45$  min) modulations of magnetospheric pulsations. Huang *et al.* [2000, 2001] reported periodic (40–60 min) perturbations in the magnetosphere and ionosphere during northward interplanetary magnetic field (IMF). A period of the order of 1 hour is longer than almost all characteristic time scales of the magnetosphere, in particular in the regions of short magnetic field lines. The generation of these long-period perturbations is not well understood.

[3] Lowest-frequency waves in the magnetosphere have been referred to as the ultra-low-frequency (ULF) magneto-hydrodynamic waves (for a review, see Hughes [1994]). Lanzerotti *et al.* [1973, 1975] reported that solar wind pressure impulses could cause excitation of ULF waves on the plasmapause and at density gradients inside the plasmasphere. Samson *et al.* [1992] and Walker *et al.* [1992] presented observations and interpretation of some discrete frequencies between 1.3 and 3.4 mHz (periods 5–13 min). Fundamental field-line resonances have frequencies just above 1 mHz. Rankin *et al.* [2000] showed that field line stretching can lead to much lower resonance frequencies. The field-line resonance frequency in a stretched magnetosphere is 1–4 mHz at latitudes corresponding to dipole *L*-shells between 6 and 10, while the frequencies calculated for the dipole magnetosphere on these *L*-shells are larger by an order of magnitude. Lui and Cheng [2001] showed that the stretching of field lines depends on magnetic activity. A field line originating at a magnetic latitude of  $68^\circ$  on the Earth's surface intersects the equatorial plane at  $X_{\text{gsm}} = -6 R_E$  for  $Kp = 1$  and at  $X_{\text{gsm}} = -20 R_E$  for  $Kp = 7$ , and the frequency of the shear Alfvén wave is reduced from 33.6 mHz at  $X_{\text{gsm}} = -6 R_E$  to 0.77 mHz at  $X_{\text{gsm}} = -20 R_E$ . It should be noted that the field line resonance frequency also depends on the cold plasma density distribution along the magnetic flux tube. The actual observed frequency at any given time may be different from

<sup>1</sup>Haystack Observatory, Massachusetts Institute of Technology, Westford, Massachusetts, USA.

<sup>2</sup>Los Alamos National Laboratory, Los Alamos, New Mexico, USA.

<sup>3</sup>Danish Meteorological Institute, Copenhagen, Denmark.

<sup>4</sup>Indian Institute of Astrophysics, Bangalore, India.

<sup>5</sup>Department of Earth and Planetary Sciences, Kyushu University, Fukuoka, Japan.

<sup>6</sup>Center for Atmospheric Research, University of Massachusetts, Lowell, Massachusetts, USA.

the calculated one if the plasma density distribution is different.

[4] An external source of longer-period magnetospheric perturbations may be in the solar wind. An increase or decrease in the solar wind pressure will compress or decompress the magnetosphere and result in a similar variation in the magnetospheric magnetic field strength. *Sibeck et al.* [1989] and *Korotova and Sibeck* [1995] found that magnetic pulsations with periods 8–10 min measured by geosynchronous satellites were well correlated with oscillations in the solar wind dynamic pressure. *Erlandson et al.* [1991], *Korotova et al.* [1997], and *Thorolfsson et al.* [2001] reported that transient variations of the solar wind pressure with a recurrent period of 30–50 min caused similar variations in the dayside magnetospheric magnetic field. *Kepko et al.* [2002] emphasized periodic variations of the solar wind pressure and their effects on the magnetosphere. They performed a spectral analysis of the upstream solar wind density/pressure and the magnetospheric magnetic field at geosynchronous orbit. They identified similar discrete spectral peaks at 0.4–2.7 mHz (6–42 min in period) in both the solar wind pressure and magnetospheric magnetic field and suggested that the discrete ULF pulsations within the magnetosphere are sometimes directly driven by oscillations in the solar wind density (or dynamic pressure). *Huang et al.* [2002] showed that periodic (~60 min) solar wind pressure oscillations caused magnetospheric and ionospheric oscillations on both the dayside and nightside.

[5] In the inner magnetosphere there is a specific type of oscillations associated with the ring current energetic particles. Periodic variations of fluxes of energetic particles have been observed at geosynchronous orbit and referred to as drift echoes. *Lanzerotti et al.* [1967] first reported ATS-1 satellite observations of such a phenomenon. Periodic oscillations occur in the electron counting rate. The period of the oscillations is a function of electron energy. The decay of the oscillations is interpreted as the result of dispersion because electrons of different energies will lose coherence while circling the Earth. Similar drift echoes are also observed in proton fluxes [*Lanzerotti et al.*, 1971]. There are two possible origins of the drift echoes. One is related to a sudden compression of the magnetosphere, as proposed by *Brewer et al.* [1969], and the other is related to impulsive injections of plasma from the magnetotail. *Chanteur et al.* [1977] analyzed ~60 electron drift echo events from ATS-5 satellite data and found that all the drift echoes were the consequence of compressions or expansions of the magnetosphere, supportive of the theory of *Brewer et al.* In contrast, *Belian et al.* [1978, 1981] studied a number of proton drift echo events observed by the Los Alamos particle analyzer instruments on the 1976-059A satellite and concluded that all the drift echoes were associated with substorm activity. *Reeves et al.* [1990] reported a drift echo event in association with substorm injections. These papers concentrated on the drift echoes but did not investigate whether the drift echoes are related to corresponding magnetospheric and ionospheric perturbations.

[6] In this paper we present geosynchronous satellite measurements of oscillations of energetic particles in the ring current region with periods of ~1 hour associated with a compression of the magnetosphere by a solar wind

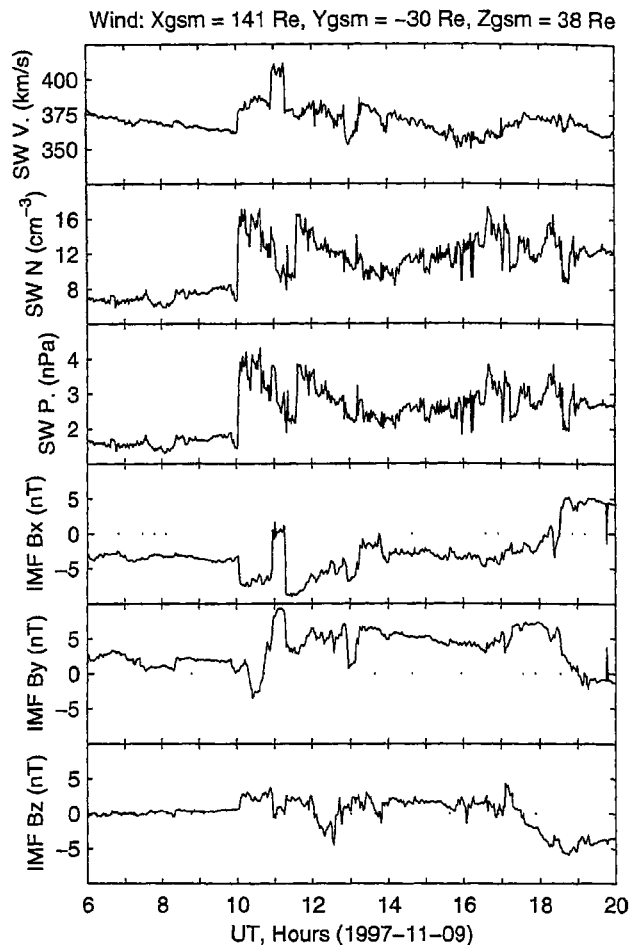


**Figure 1.** Solar wind (SW) velocity, solar wind ion density, solar wind pressure, and interplanetary magnetic field (IMF) components in GSM coordinates measured by the Wind satellite on 9 November 1997. A solar wind pressure impulse is registered by Wind at 1002 UT. The position of Wind at 1002 UT is given at the top of the figure.

pressure impulse. Periodic magnetic perturbations are detected by ground magnetometers from the auroral to equatorial latitudes on the dayside and nightside. These observations may represent global magnetospheric-ionospheric oscillations. We will discuss the possible mechanisms which are responsible for the generation of the magnetospheric oscillations.

## 2. Observations

[7] The event in the present study occurred during magnetically quiet times on 9 November 1997. The IMF  $B_z$  was northward or near zero between 0000 UT on 8 November and 1730 UT on 9 November, and the  $K_p$  index was smaller than 3-. Figure 1 shows, from top to bottom, the solar wind velocity, solar wind ion density, solar wind dynamic pressure, and IMF components measured by the Wind satellite between 0600 and 2000 UT on 9 November 1997. A solar wind pressure impulse is registered by Wind at 1002 UT; the pressure jumps from 1.5 nPa at 1002 UT to ~4.0 nPa at 1010 UT. The solar wind ion

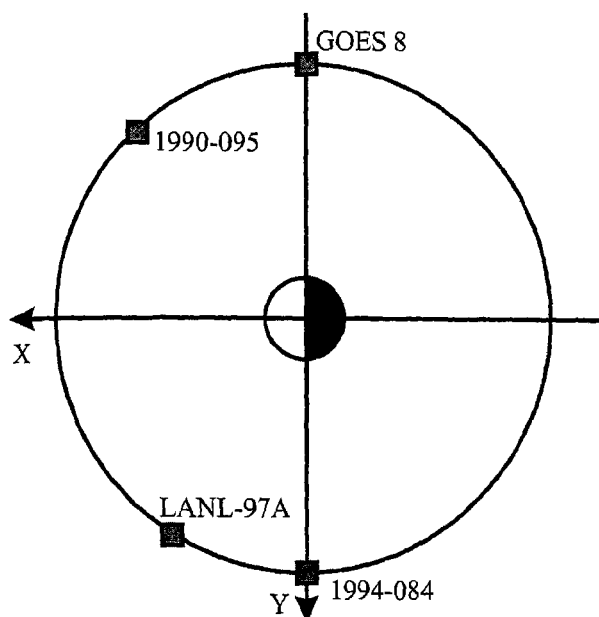


**Figure 2.** Positions of geosynchronous satellites GOES 8, 1990-095, LANL-97A, and 1994-084 in the magnetospheric equatorial plane at 1043 UT, corresponding to the arrival of the solar wind pressure impulse at the magnetosphere. The shaded squares represent the satellites. The positive direction of the  $X$  axis is toward the Sun, and the positive  $Y$  direction is toward dusk.

density increases from  $6 \text{ cm}^{-3}$  at 1002 UT to  $17 \text{ cm}^{-3}$  at 1010 UT; the pressure change is mainly determined by the density change. Sudden variations also occur in three IMF components at this moment.

[8] The solar wind velocity is  $\sim 380 \text{ km/s}$  after the pressure impulse. The solar wind would take  $\sim 40 \text{ min}$  to propagate from the Wind position to the Earth. As will be shown later, the solar wind pressure impulse influences the magnetosphere at 1043 UT, indicating an actual time delay of 41 min. We present data measured by four geosynchronous satellites, the Geostationary Operational Environmental Satellite GOES 8 and the Los Alamos National Laboratory satellites LANL-97A, 1994-084, and 1990-095, to show the effects of the solar wind pressure impulse on the magnetosphere. All the geosynchronous satellites are close to the equatorial plane, with a radial distance of  $\sim 6.6 R_E$ . Magnetic local time (MLT) is about UT - 5 hours at GOES 8, UT - 2 hours at 1990-095, UT + 5 hours at LANL-97A, and UT + 7 hours at 1994-084. Figure 2 displays the locations of the four satellites at 1043 UT: GOES 8 at  $\sim 0600 \text{ MLT}$ , 1990-095 at  $\sim 0850 \text{ MLT}$ , LANL-97A at  $\sim 1550 \text{ MLT}$ , and 1994-084 at  $\sim 1800 \text{ MLT}$ . These satellites have a large separation along longitude/local time.

[9] Figure 3 shows the magnetospheric magnetic field measured by GOES 8. The magnetic field is given in the local coordinate system. The magnetic field  $H_p$  component is perpendicular to the satellite orbital plane (or nearly northward),  $H_e$  is earthward, and  $H_n$  is eastward. In the geosynchronous orbit near the equatorial plane,  $H_p$  is the main component of the field. When GOES 8 moves from nightside toward dawn between 0900 and 1042 UT, the

magnetic field increases gradually. Then the vertical component  $H_p$  starts to increase rapidly from 105 nT at 1043 UT to 119 nT at 1053 UT. The radial component  $H_e$  decreases from 49 nT at 1043 UT to 45 nT at 1057 UT. The timing of the rapid changes in  $H_p$  and  $H_e$  is consistent with the expected arrival of the solar wind pressure impulse. When the magnetosphere is compressed by a solar wind pressure impulse, the dayside magnetic field lines become more vertical. The observed increase in  $H_p$  and decrease in  $H_e$  are consistent with the compressional effect. After the compression, the  $H_n$  component shows perturbations with a mean period of  $\sim 45 \text{ min}$  before 1330 UT. In contrast, the magnetospheric-ionsospheric oscillations that will be discussed below have a mean period of  $\sim 1 \text{ hour}$ . It is not clear what causes the perturbations in the magnetic field  $H_n$  component.

[10] We present in Figure 4 the energetic particle fluxes measured by the Synchronous Orbit Particle Analyzer (SOPA) instruments onboard the LANL-97A, 1994-084, and 1990-095 satellites. The left column shows electron fluxes, and the right column shows proton fluxes. No proton flux data are available from 1990-095. A prominent feature in Figure 4 is that all three satellites detect a sudden flux increase in all energy channels simultaneously at 1043 UT. This implies that the compressional front is global and propagates quickly in the magnetosphere by the fast mode wave, so the compression is sensed by satellites at widely separated local times. After the first increase, enhancements in particle fluxes at different energy channels show different periods, with longer periods for particles of lower energies. The temporal variation and energy dispersion of the fluxes are similar to those in previous observations [Lanzerotti, 1967, 1971; Chanteur *et al.*, 1977; Belian *et al.*, 1978, 1981; Reeves *et al.*, 1990]. It is important to note that the strongest oscillations in electron fluxes occur in the middle three channels of 75–105, 105–150, and 150–225 keV.

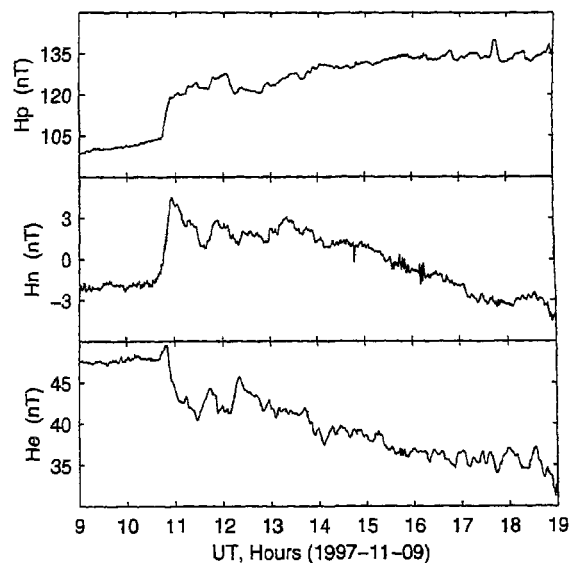


**Figure 3.** Magnetospheric magnetic field measured by the GOES 8 satellite. The rapid increase of the  $H_p$  component at 1043 UT indicates a sudden compression of the magnetosphere.

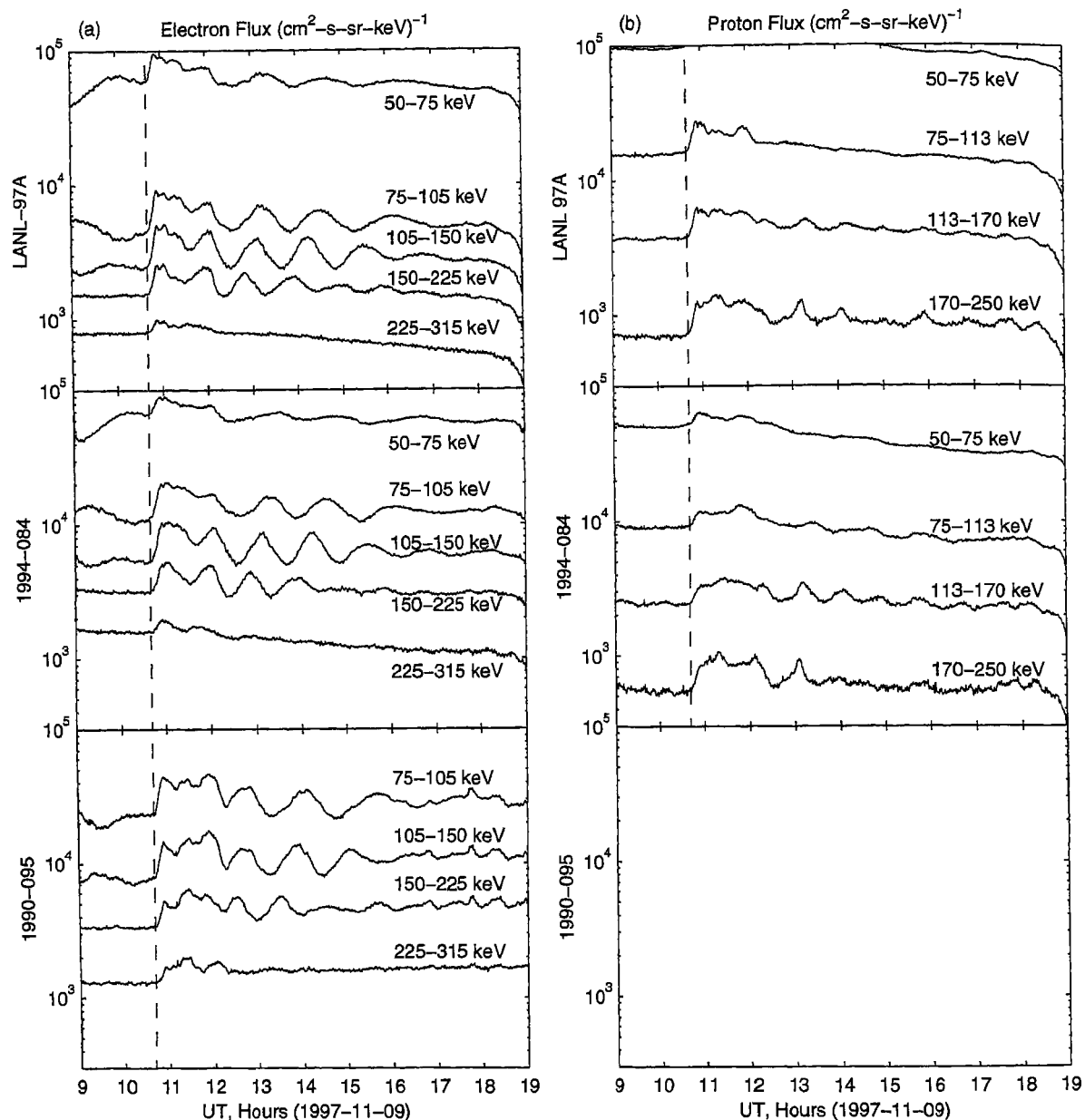


**Figure 4.** Magnetospheric particle fluxes measured by the geosynchronous satellites LANL-97A, 1994-084, and 1990-095. The first flux enhancement at 1043 UT is observed simultaneously at different longitudes (local times), as indicated by the vertical dashed line. The strongest oscillations of the electron fluxes occur in the three middle energy channels.

These oscillations last for  $\sim 7$  hours until  $\sim 1800$  UT. Oscillations are very weak at higher and lower energies. The oscillations of the protons are much weaker than those from electrons. The SOPA instruments have logarithmically spaced energy channels so that the count rates in each channel are approximately the same even though the fluxes decrease with increasing energy (for details of the instruments, see *Belian et al.* [1992]). The channels get wider with increasing energy, leading to a broader range of drift periods within a given channel at high energies. That does not effect the chance of seeing echoes since they should still show up at the period of the lowest energy in the channel. It appears that there is a particular characteristic frequency of

the magnetospheric disturbances that resonate with the drift period of particles of a particular energy. Channels with drift periods that put them in near resonance have sustained pulsations. Channels with energies that are too high or too low do not resonate as coherently and do not sustain pulsations.

[11] In the present case the first enhancement of the fluxes at 1043 UT coincides exactly with the compression of the magnetosphere. Such a flux enhancement simultaneously over a large longitudinal/local time sector is different from substorm injections. During substorms, energetic particles are injected to the geosynchronous orbit from nightside [*Belian et al.*, 1978, 1981; *Reeves et al.*, 1990, 1998]. After

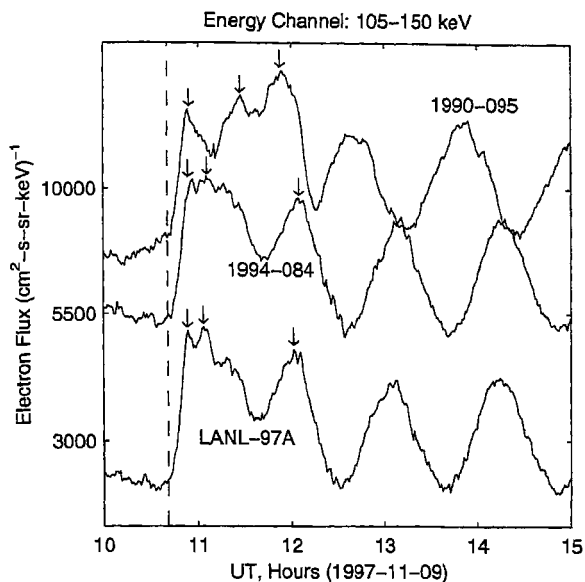


**Figure 5.** Electron fluxes in the energy channel 105–150 keV measured by LANL-97A (the bottom curve), 1994-084 (the middle curve), and 1990-095 (the top curve). The vertical dashed line at 1043 UT indicates that the fluxes start to increase. The arrows indicate peaks of fluxes.

being injected, protons drift westward and electrons drift eastward. The first flux enhancement of electrons and protons with different energies reach different longitudes at different times for substorm injections.

[12] We plot in Figure 5 the electron fluxes in energy channel 105–150 keV. Note that at this moment 1990-095 is at  $\sim 0850$  MLT, LANL-97A is at  $\sim 1550$  MLT, and 1994-084 is at  $\sim 1800$  MLT (Figure 2). For each satellite's data, three arrows are used to indicate the first three peaks of the flux enhancements. The vertical dashed line at 1043 UT indicates the time at which the fluxes start to increase. The fluxes reach the first peak value at  $\sim 1053$  UT at the locations of the three satellites, indicating a global compression of the magnetosphere. The second peak may be related to the changes in the magnetic topology and particle distribution after the magnetosphere is suddenly compressed. From the third flux peak the flux variations become very regular and periodic. Spacecraft 1990-095 is nearly a half period out of phase with 1994-084 which is consistent with their locations almost 180 degrees apart in longitude. The phase delay is consistent with particle drift, and the timing is also consistent with eastward drift of the electrons. Since the magnetosphere is compressed on the dayside, we expect that the flux enhancement is the greatest near local noon. The periodic variations of the fluxes may represent a day-night asymmetry of the electron distribution, and the whole asymmetric pattern drifts eastward. A full cycle of the drifting motion corresponds to a full circumference of the Earth. If we use a wave to describe the oscillations, the wave has a mode number equal to one. *Lessard et al.* [1999] found that monochromatic magnetospheric pulsations were modulated with a 45-min periodicity and that the pulsations had an azimuthal wave number of  $\sim 1$ . They suggested that a global perturbation induces a radially polarized electric field that results in the flux modulations of energetic

electrons at geosynchronous orbit. Some link may exist between the global perturbation in the event of Lessard and the magnetospheric oscillations initiated by a solar wind pressure impulse reported in the present paper.

[13] Because the velocity of the curvature/gradient drift of electrons depends on energy, the period of the energetic particle oscillations varies with energy. Therefore the flux peaks after the first compression show time lags at different locations. We can directly find the drift periods from successive positive and negative peaks of the fluxes; the results are plotted in Figure 6. The solid line represents the least-squares fit of the data. For the three energy channels with the strongest oscillations, the periods are 55–80 min. The periods that are observed are all within a factor of 1.5 of 60 min, which is suggestive of resonance with a fixed-period driving wave. The periodicity may be driven by a wave that is nearly in resonance but the electrons are “bunched” in their drift orbit. The observed periods of the flux variations coincide well with the calculations of *Schulz and Lanzerotti* [1974].

[14] The above geosynchronous satellite observations show the magnetospheric perturbations caused by the solar wind pressure impulse. We now turn to ground observations in order to find what happens in the ionosphere. The names and locations of the magnetometers used in the present study are listed in Table 1. Ground magnetometers measure magnetic deviations which result from changes in ionospheric currents. Figure 7 shows the magnetic deviations at the auroral latitudes detected by the Greenland west coast magnetometer chain and by the Canadian Auroral Network for the OPEN Program United Study (CANOPUS) magnetometer array. We are interested in long-period oscillations with periods ( $\sim 1$  hour) and have used a low-pass (30 min) filter to remove rapid fluctuations. In Figure 7, only the

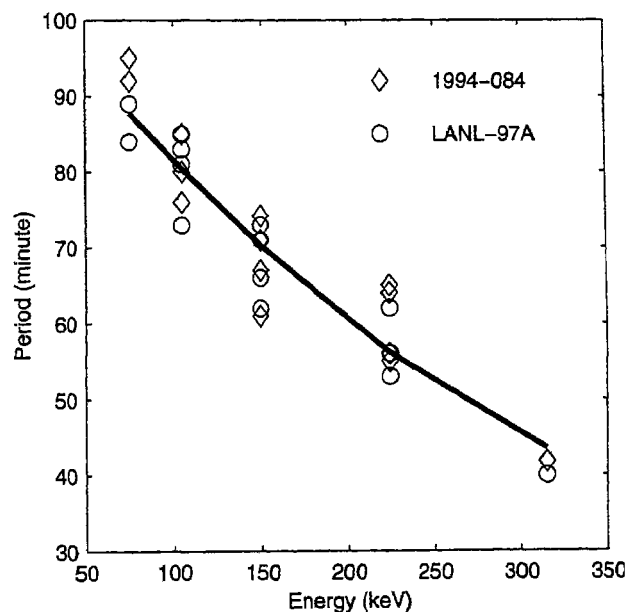


**Figure 6.** Period of the flux enhancements as a function of energy. The diamonds represent the data measured by 1994-084, and the circles represent the data measured by LANL-97A. The solid line is the result of a least-square fit.

**Table 1.** Locations of Ground Magnetometers

Stations	Abbreviations	Geographic		Geomagnetic	
		Long.	Lat.	Long.	Lat.
<i>Greenland Magnetometers</i>					
Attu	ATU	306.4	67.9	39.0	74.7
Maniitsoq	SKT	307.1	65.4	37.8	72.1
Nuuk	GHB	308.2	64.1	38.5	70.7
Paarmiut	FHB	310.3	62.0	39.6	68.1
Narsarsuaq	NAQ	314.5	61.1	43.9	66.4
<i>CANOPUS Magnetometers</i>					
Rankin Inlet	RANK	267.8	62.8	331.0	73.5
Eskimo Point	ESKI	265.9	61.1	328.4	71.8
Fort Churchill	FCHU	265.9	58.7	329.2	69.5
Island Lake	ISLL	265.3	53.8	329.6	64.7
Pinawa	PINA	263.9	50.2	328.4	61.0
<i>STEP 210 (deg) Magnetometers</i>					
Magadan	MGD	150.8	59.9	218.7	53.5
Moshiri	MSR	142.2	44.3	213.3	37.6
Lumping	LNP	121.1	25.0	189.5	13.8
Learmonth	LMT	114.1	-22.2	185.1	-33.5
Canberra	CAN	149.0	-35.3	226.2	-45.9
Muntinlupa	MUT	121.0	14.3	192.2	6.3
Biak	BIK	136.0	1.0	207.3	-9.7
Guam	GAM	144.8	13.5	215.5	5.6
Ancon	ANC	282.8	-11.7	354.4	3.0
Eusebio	EUS	321.5	-3.8	34.7	0.1

eastward component of the magnetic deviations is shown because the deviations are most obvious in this component. The Greenland magnetometer data are presented in local magnetic coordinates, and the CANOPUS data are presented

in geographic coordinates. Three major oscillations occur at  $\sim 1100$  UT,  $\sim 1200$  UT, and  $\sim 1300$  UT in the Greenland magnetometers. In the CANOPUS magnetometer data, similar oscillations with a period of  $\sim 1$  hour occur between 1100 and 1500 UT. MLT at the Greenland west coast magnetometers is about UT - 2.5 hours, and MLT at the CANOPUS magnetometers is about UT - 7 hours. During the period of interest the Greenland magnetometers are in the noon sector, and the CANOPUS magnetometers are in the morning sector. The perturbations of the auroral ionospheric currents are caused by the ionospheric conductivity and/or electric fields which, in turn, are related to magnetospheric particle precipitation and electric fields. Since the magnetometers between  $60^\circ$  and  $70^\circ$  magnetic latitudes might be equatorward of the auroral zone on the dayside when the IMF  $B_z$  is mostly positive, we expect that particle precipitation may be not significant. Thus the variations in the ionospheric currents are interpreted as the consequence of electric fields originating from the magnetosphere.

[15] If the magnetospheric electric fields penetrate into the low-latitude ionosphere, the electric fields will result in similar ionospheric disturbances at low latitudes too. The ionospheric currents at low latitudes are mainly in the east-west direction. Variations in the eastward current will cause corresponding variations in the northward component of magnetic deviations. Figure 8a displays the northward ( $H$ ) component of magnetic field deviations measured by the ground magnetometers of the Solar-Terrestrial Energy Program (STEP) 210 (deg) magnetic meridian chain around geographic longitudes  $110^\circ$ – $140^\circ$ . The deviations in the

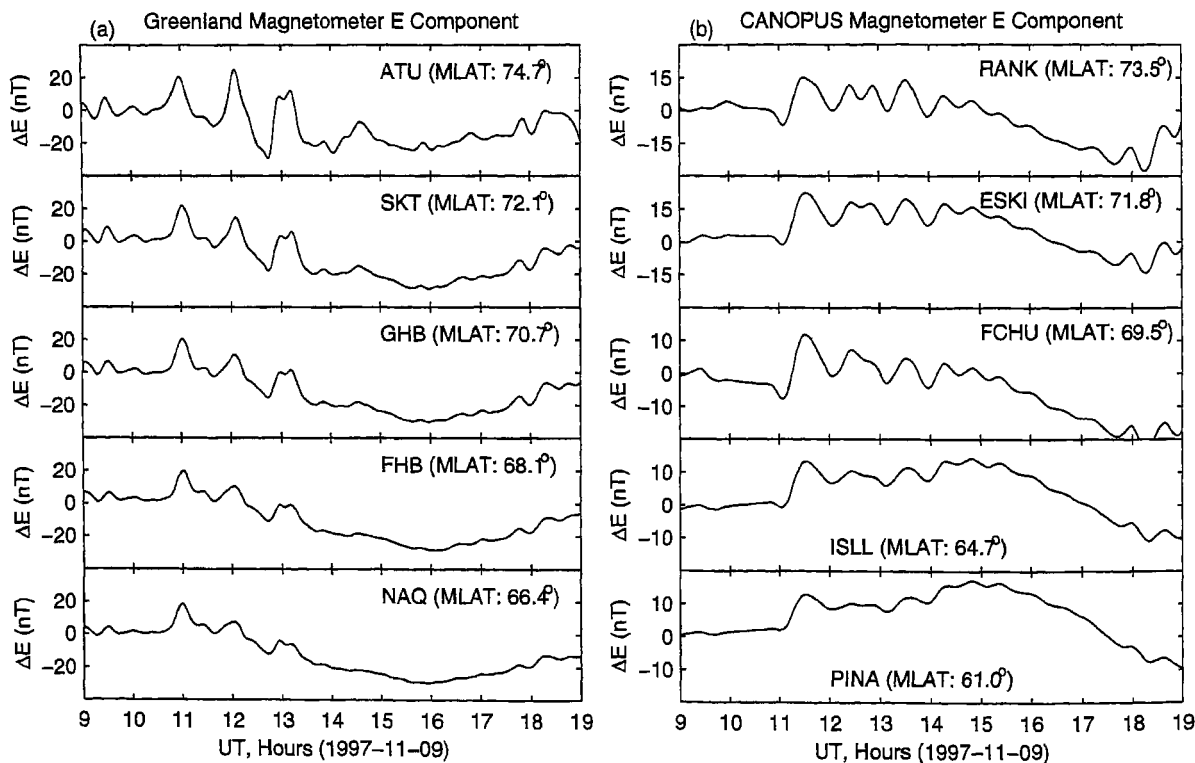


**Figure 7.** The eastward component of magnetic field deviations measured by ground magnetometers at ATU, SKT, GHB, FHB, and NAQ in the Greenland chain, and RANK, ESKI, FCHU, ISLL, and PINA in the CANOPUS chain. Geomagnetic latitude (MLAT) is given in the parenthesis after each station. Periodic oscillations start to occur at  $\sim 1043$  UT.

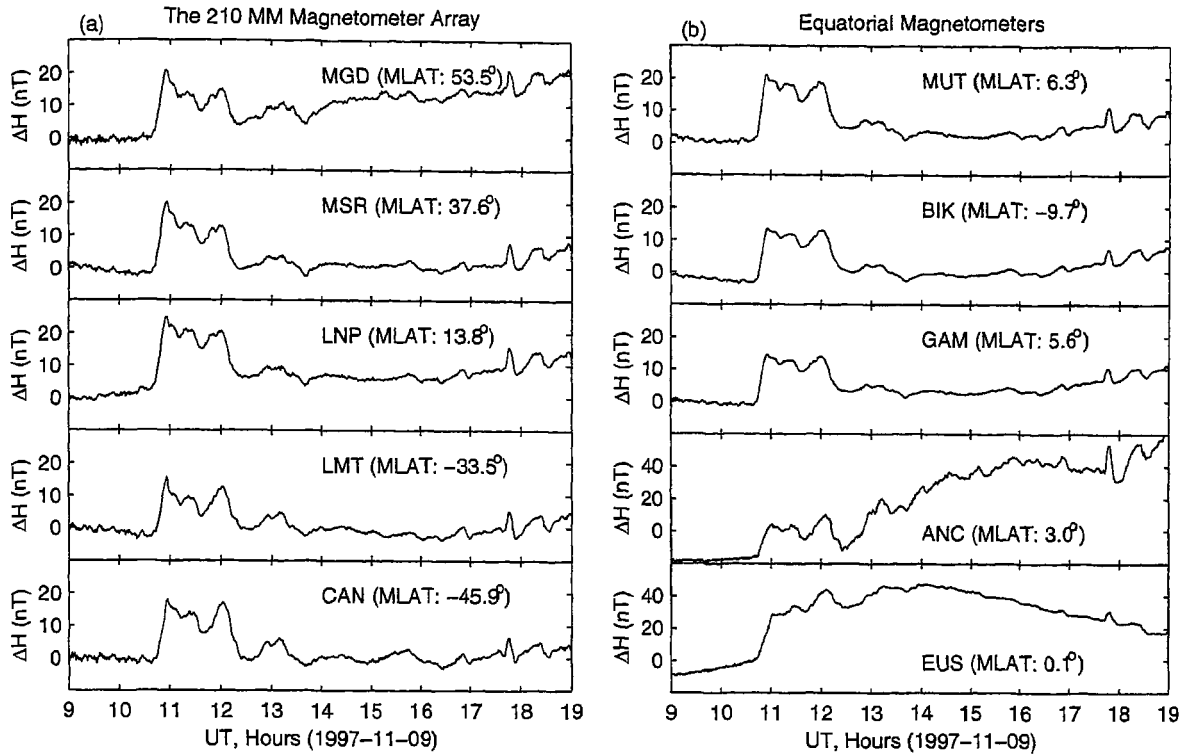


**Figure 8.** The northward component of ground magnetic field deviations measured by the STEP magnetometers at MGD, MSR, LNP, LMT, and CAN along magnetic longitude  $\sim 210^\circ$ , and MUT, BIK, GAM, ANC, and EUS along the magnetic equator. Geomagnetic latitude (MLAT) is given in the parenthesis after each station. Periodic oscillations start at  $\sim 1043$  UT.

$D$  and  $Z$  components are much weaker and are not plotted. MGD, MSR, and LNP are located in the Northern Hemisphere, and LMT and CAN are in the Southern Hemisphere. Figure 8b shows measurements from magnetometers very close to the magnetic equator. MUT, BIK, and GAM are stations of the 210 MM array in Asia; ANC and EUS are in South America. All the magnetometers detect a sudden increase in the magnetic field around 1043 UT. Then the magnetic deviations become periodic with a period of  $\sim 1$  hour. Compared with Figure 7, the magnetic deviations at lower and equatorial latitudes start at the same time as the auroral magnetic deviations, indicating that the magnetospheric electric fields might indeed penetrate into the global ionosphere from high to equatorial latitudes. It should be noted that the periodic magnetic deviations are clearer in the auroral zone than those at lower latitudes. Perhaps the source of the disturbances is located at high latitudes. This issue will be further discussed later.

[16] It is known that oscillations in the solar wind pressure and IMF can result in similar oscillations in the magnetosphere and ionosphere [Huang *et al.*, 2002]. In order to identify whether the period of the magnetospheric and ionospheric oscillations in the present case is determined by the solar wind, we make a comparison of some parameters. In Figure 9a we plot the solar wind pressure, the IMF  $B_z$  component, the LANL-97A electron flux in the energy channel of 105–150 keV, the  $E$  component of the Greenland FHB magnetometer at geographic longitude  $310^\circ$  in the Northern Hemisphere, and the  $H$  component of Australian LMT magnetometer at geographic longitude  $114^\circ$  in the

Southern Hemisphere. The magnetometer data in Figure 9 are not detrended in order to show clearly the timing. The solar wind pressure and IMF  $B_z$  data have been shifted by 41 min, which is the propagation delay from the Wind position to the magnetosphere. After the shift, the solar wind pressure impulse coincides well with the first enhancement in the LANL-97A electron flux and ground magnetic deviations at  $\sim 1043$  UT, indicating the solar wind initiation of the magnetospheric-ionospheric oscillations. After 1043 UT the magnetospheric and ionospheric parameters show periodic oscillations. However, the solar wind pressure and IMF  $B_z$  do not show corresponding variations. An important feature of Figure 9a is that the magnetospheric and ionospheric oscillations have a clear period of  $\sim 1$  hour and that the solar wind pressure and IMF  $B_z$  do not have this periodicity.

[17] In Figure 9b the data are plotted in an expanded time scale. Obviously, the compression of the magnetosphere, represented by the  $H_p$  component of the GOES 8 measurement, starts at 1043 UT. The LANL-97A electron flux starts to increase exactly at this moment. GOES 8 and LANL-97A are separated by  $\sim 10$  hours in local time (Figure 2). The simultaneous occurrence of the magnetosphere compression and flux enhancement indicates the global characteristic of the perturbations. The ground magnetometer deviations show some subtle differences. At 1043 UT, FHB of the Greenland chain and FCHU of the CANOPUS chain are in the dawn-morning sector, and LMT and MUT of the 210 MM magnetometer array are in the evening sector. The magnetic deviations at LMT and MUT start to increase at 1043 UT. However, the magnetic deviation at FHB starts to

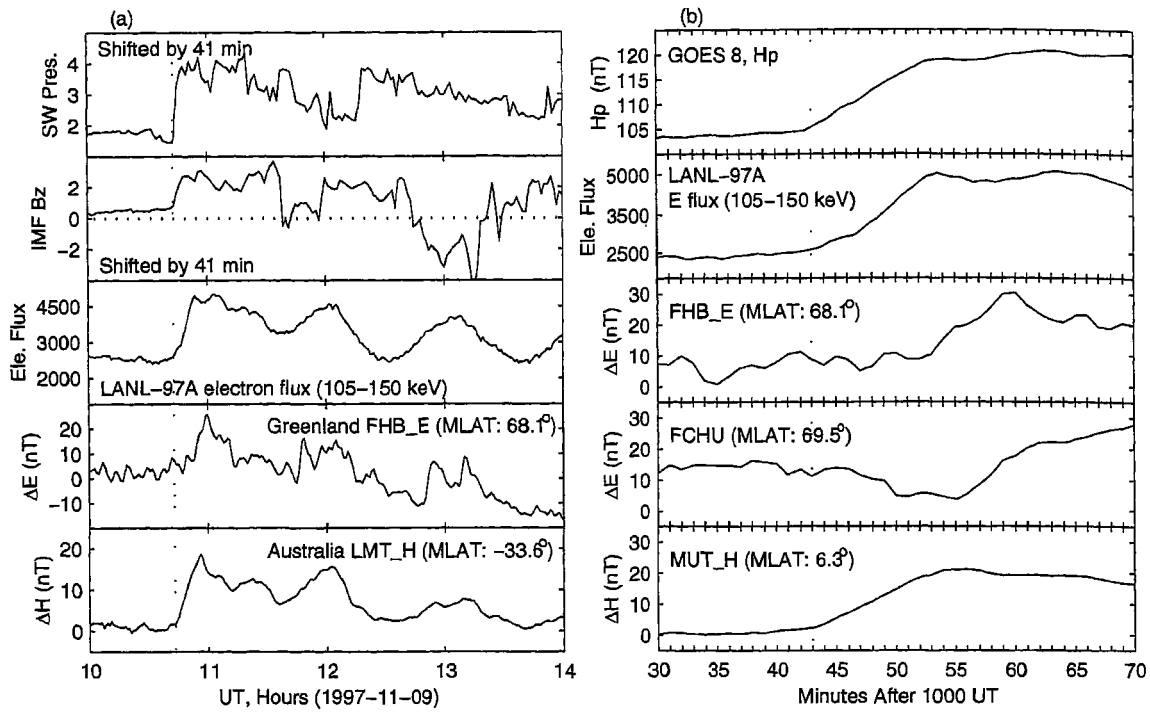


**Figure 9.** Timing and evolution of perturbations in the solar wind, magnetosphere, and ionosphere. The magnetospheric-ionospheric perturbations start at ~1043 UT, as indicated by the vertical dotted line. Geomagnetic latitude (MLAT) is given in the parenthesis after each magnetometer station.

increase noticeably at 1053 UT, and the magnetic deviation at FCHU shows a decrease during 1046–1055 UT and then an increase.

[18] The difference between the solar wind and ionosphere can be also seen from a spectral analysis. In Figure 10a the

spectral power of the IMF  $B_z$  component, solar wind ion density, and solar wind dynamic pressure between 0820 and 1520 UT is plotted. All three solar wind parameters show the same peak at a period of 90 min. Such a period is readily seen in Figure 9a. The solar wind pressure shows clearly

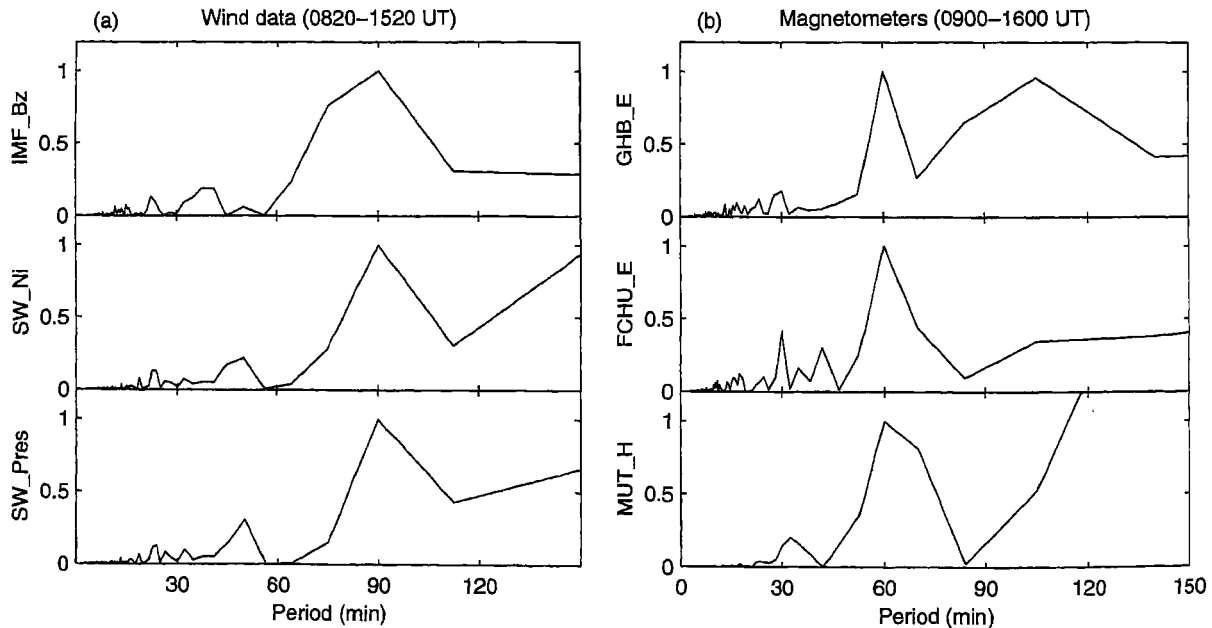


**Figure 10.** (a) Normalized spectral power of the IMF  $B_z$ , solar wind ion density, and solar wind pressure during 0820–1520 UT, and (b) the Nuuk (GHB) magnetometer  $E$  component of the Greenland chain, Fort Churchill (FCHU) magnetometer  $E$  component of the CANOPUS chain, and Muntinlupa (MUT) magnetometer  $H$  component of the 210 MM chain during 0900–1600 UT.

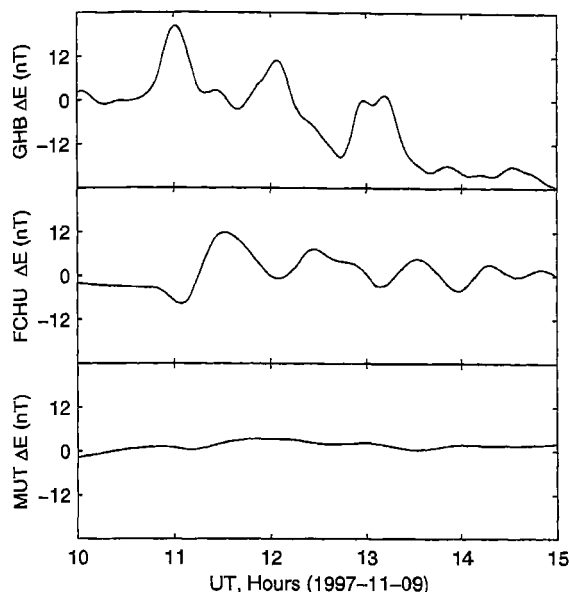


**Figure 11.** Comparison of magnetic deviations at Nuuk (GHB, geographic 308.2°E, 64.1°N, geomagnetic 38.5°E, 70.7°N), Fort Churchill (FCHU, geographic 265.9°E, 58.7°N, geomagnetic 329.2°E, 69.5°N), and Muntinlupa (MUT, geographic 121.0°E, 14.3°N, geomagnetic 192.2°E, 6.3°N).

two cycles of variations between 1040 and 1340 UT, and the IMF  $B_z$  turns northward around 1040, 1200, and 1340 UT. The solar wind ion density has the same temporal variations as the pressure. In contrast, the ground magnetometers have a major spectral peak at a period of 60 min, as shown in Figure 10b. Since the solar wind would take  $\sim 40$  min to travel from the Wind position to the magnetosphere, the spectral analysis of the magnetometers are taken between 0900 and 1600 UT. We only plot the spectrum of one magnetometer for each magnetometer chain. It is clear from Figures 7 and 8 that all other magnetometers show a similar period of  $\sim 60$  min.

[19] Although the ground magnetometer deviations at different longitudes have the same periodicity of 60 min, their phase and amplitude are different. We plot in Figure 11 the  $E$  component of the magnetic field deviations at GHB of the Greenland west coast chain, FCHU of the CANOPUS chain, and MUT of the 210 MM chain. A low pass (30 min) filter has been applied to the data. The phase of the perturbation at FCHU is almost exactly opposite to that of the perturbation at GHB. At the equator (MUT), the  $E$  component perturbation becomes very small and unidentifiable. Figures 7 and 8 show that the magnetic deviations at each magnetometer chain (the Greenland chain, the CANOPUS chain, or the 210 MM chain) have the same phase. Therefore the phase difference must represent the variations along longitude (or local time).

### 3. Discussion

[20] The prominent feature in the magnetospheric-ionospheric oscillations presented in this paper is the occurrence of the period of  $\sim 60$  min. As discussed in section 1,

variations in the solar wind may result in similar variations in the magnetosphere and ionosphere. Such a correspondence between the solar wind and magnetosphere has been identified [Sibeck *et al.*, 1989; Korotova and Sibeck, 1995; Erlandson *et al.*, 1991; Korotova *et al.*, 1997; Thorolfsson *et al.*, 2001]. In particular, Kepko *et al.* [2002] and Huang *et al.* [2002] have found that periodic (40–60 min) oscillations in the solar wind pressure can cause oscillations with the same period in the magnetosphere and ionosphere. However, as displayed in Figures 9 and 10, the time series and spectrum analyses show that the solar wind does not have the same period as that in the magnetosphere and ionosphere in the present case, and therefore we have to exclude the solar wind as a direct driving source of the 60-min periodicity in the magnetospheric-ionospheric oscillations.

[21] If the period of  $\sim 60$  min is not caused by an external source, it must be determined by the magnetospheric-ionospheric system. A field-line resonance is generally thought to be the lowest frequency of a disturbance that is inherent to the magnetosphere. Samson *et al.* [1971] and Samson [1972] found that Pc 5 pulsations (periods of 5–15 min) had maximum intensity around magnetic latitude 67°, and the pulsation intensity became lower toward both higher and lower latitudes. The latitude of maximum intensity moved to the south for higher-frequency pulsations and to the north for lower-frequency pulsations. Hughes [1974] showed that the polarization of a magnetospheric disturbance associated with field line resonance will be rotated through a right angle when it is seen on the ground because of the effect of the ionospheric current sheets. If the magnetospheric disturbance is linearly polarized North-South, the polarization on the ground will be linear East-West.

[22] In our case the ground magnetometer deviations were larger at higher latitudes, as shown in Figure 7. If they were caused by field line resonance, the resonance might occur at magnetic latitude 74° or higher. Lui and Cheng [2001] showed that the frequency of the ULF wave on field lines originating at a magnetic latitude of 68° on the Earth's surface in a stretched magnetosphere is 0.77 mHz (period of 21.6 min). It is not certain whether the field lines originating at magnetic latitude 74° or higher could have a resonant period of  $\sim 60$  min. Perhaps a disturbance electric field associated with some tail perturbations penetrated to the ionosphere and caused variations in the low-latitude ionospheric currents. Since the ionospheric currents at low latitudes are mainly in the east-west direction, the resulting magnetic deviations are in the north-south direction. Lessard *et al.* [1999] observed magnetospheric-ionospheric perturbations with a period of  $\sim 45$  min. It is the east-west component of ground magnetometer deviations at the south pole (high latitudes) that showed a good correlation with magnetospheric pulsations in their case. They also invoked a global disturbance electric field to interpret inner-magnetospheric perturbations.

[23] However, some important problems remains unsolved. Further theoretical and simulation studies are required to verify whether the magnetospheric tail can support resonance periods of 45–60 min. We also need to understand how a tail disturbance reaches the inner magnetosphere and lower-latitude ionosphere.

[24] As shown in Figure 9, all the magnetospheric and ionospheric oscillations were excited in association with the compression of the magnetosphere. It is reasonable to

assume that the solar wind pressure impulse initiated the oscillations in the magnetosphere and ionosphere. After the initiation the solar wind may no longer play a role in the subsequent evolution of the magnetospheric-ionospheric oscillations. The key point of the interpretation is that the period of the magnetospheric-ionospheric oscillations is intrinsic to the magnetosphere-ionosphere system and is determined solely by this system. The solar wind pressure impulse is to trigger or excite the magnetospheric oscillations but does not determine the period of the oscillations.

[25] When the magnetosphere oscillates, a resonance is most easily excited for electrons whose drift periods are close to the magnetospheric oscillation period. As shown in Figure 4, the strongest electron oscillations occur in the energy channels of 75–105, 105–150, and 150–225 keV and have periods 55–80 min. The oscillations with higher and lower energies are much weaker because their drift motion does not match the resonance with the magnetosphere. The oscillations in the present event result from particle bunching due to the compression of the dayside magnetosphere by the solar wind pressure impulse. They do not result from particle injections from the tail during substorms, so their period is not related to substorm cycles.

[26] The above interpretation is consistent with other observations. *Huang et al.* [2001] reported observations of periodic ( $\sim 1$  hour) perturbations in the magnetosphere and ionosphere during a 29-hour interval of northward IMF. They suggest that the magnetosphere is largely closed for such a prolonged northward IMF and that the period of the oscillations is determined by the length of the tail (or the magnetosphere). Recently, *Huang* [2002] has studied the relationship between the solar wind and periodic magnetospheric substorms. Periodic (2–3 hour) near-tail magnetic reconnection and plasmoids are detected at  $X_{\text{gsm}} = -22 \sim -30 R_E$  by the Geotail satellite and that these typical substorm signatures can occur for many cycles without significant attenuation. *Huang et al.* [2003b] show that periodic (2–3 hour) energetic particle injections are measured at geosynchronous orbit; this phenomenon is termed “sawtooth injections.” The sawtooth injections may be related to the expansion phase of substorms. They suggest that the magnetospheric substorms have an intrinsic cycle time of 2–3 hours and that the role played by solar wind variations is to trigger the periodic substorms.

[27] These recent efforts are to explore whether long-period (1–3 hour) oscillations can occur in the magnetosphere and what determines the period of the oscillations. The observations show that magnetospheric oscillations have periods of  $\sim 1$  hour during quiet times (*Huang et al.* [2001] and this paper) and periods of 2–3 hours during disturbed times [*Huang*, 2002; *Huang et al.*, 2003b]. These long-period oscillations seem intrinsic to the magnetosphere because the solar wind does not show the same periodicity in these cases. It appears that a resonant state of the magnetosphere with these long periods can be excited by sudden changes in the solar wind. After the magnetosphere has become active the oscillations can continue for many cycles without requirement of continuous external forcing. These recent observations increase our understanding of magnetospheric physics and, on the other hand, put forward new challenge for magnetospheric wave theories. As mentioned in section 1, the existing theories of magnetospheric

ULF waves predict the longest wave period of  $\sim 15$  min and cannot be applied to the recently observed oscillations with periods of 1–3 hours.

[28] The Millstone Hill group has been paying attention to prompt effects of solar wind variations on the midlatitude ionosphere. *Huang and Foster* [2001] have found that a sudden decrease in the solar wind pressure causes a significant decrease of 25–30% in the dayside ionospheric *F*-region plasma density over  $37^\circ$ – $44^\circ$  geographic latitudes. *Huang et al.* [2002] have reported that variations with periods of 1–2 hours in the IMF orientation and/or solar wind pressure cause similar perturbations in the midlatitude ionosphere; the *F*-region electron density can be increased or decreased by  $\sim 30\%$  within 30–70 min. *Huang et al.* [2003a] have shown that a solar wind pressure impulse triggered periodic magnetospheric substorms during a magnetic storm and that the periodic substorms induced significant perturbations in the midlatitude ionosphere. In this paper we have shown that a solar wind pressure impulse may cause periodic magnetospheric oscillations and ionospheric perturbations from the auroral to equatorial latitudes. Our purpose is to reveal the relationship among variations in the solar wind, magnetosphere, and ionosphere. Such a relationship is very important for our understanding of the geospace environment.

#### 4. Summary

[29] We have presented the observations of magnetospheric and ionospheric oscillations associated with a solar wind pressure impulse. When the magnetosphere is suddenly compressed, enhancements in energetic electron fluxes are detected by geosynchronous satellites simultaneously over a large longitudinal range. The electron fluxes show periodic variations mainly in the energy channels of 75–105, 105–150, and 150–225 keV with periods of 55–80 min; these periodic variations are identified as the electron bunches circling the Earth. Periodic ( $\sim 1$  hour) oscillations of geomagnetic field are measured by ground magnetometers from the auroral to equatorial latitudes. The magnetospheric oscillations and the ground magnetometer perturbations start to occur simultaneously. The solar wind pressure and IMF do not show variations similar to the magnetospheric oscillations and magnetometer magnetic deviations in this case.

[30] Our interpretation of the phenomena is as follows. When the magnetosphere is suddenly compressed by the solar wind pressure impulse, intrinsic magnetospheric oscillations are excited. The solar wind plays a role in initiating the magnetospheric oscillations, while the period of the oscillations is determined by the magnetosphere itself. Under the condition of mostly northward IMF in this event the period of the magnetospheric oscillations is  $\sim 1$  hour. The drift motion of the ring-current electrons with periods close to the magnetospheric oscillation period is most readily excited, and the disturbance electric fields associated with the magnetospheric oscillations penetrate to the ionosphere and cause magnetic deviations.

[31] **Acknowledgments.** Work at MIT Haystack Observatory was supported by a NSF cooperative agreement with Massachusetts Institute of Technology. The Greenland magnetometers are operated by the Danish

Meteorological Institute. Solar-Terrestrial Environment Laboratory, Nagoya University supports construction of the 210 MM database. We thank the Canadian Space Agency for providing the CANOPUS magnetometer data and acknowledge the CDAWeb for access to the Wind and GOES 8 data. Arthur Richmond thanks the reviewers for their assistance in evaluating this paper.

## References

- Belian, R. D., D. N. Baker, P. R. Higbie, and E. W. Hones Jr., High-resolution energetic particle measurements at 6.6  $R_E$ : 2. High-energy proton drift echoes, *J. Geophys. Res.*, **83**, 4857, 1978.
- Belian, R. D., D. N. Baker, E. W. Hones Jr., P. R. Higbie, S. J. Bame, and J. R. Asbridge, Timing of energetic proton enhancements relative to magnetospheric substorm activity and its implication for substorm theories, *J. Geophys. Res.*, **86**, 1415, 1981.
- Belian, R. D., G. R. Gislser, T. Cayton, and R. Christensen, High-Z energetic particles at geostationary orbit during the great solar proton event series of October 1989, *J. Geophys. Res.*, **97**, 16,897, 1992.
- Brewer, H. R., M. Schulz, and A. Eviatar, Origin of drift-periodic echoes in outer-zone electron flux, *J. Geophys. Res.*, **74**, 159, 1969.
- Chanteur, G., R. Gendrin, and S. Perraut, Experimental study of high-energy electron drift echoes observed on board ATS 5, *J. Geophys. Res.*, **32**, 5231, 1977.
- Erlanson, R. E., D. G. Sibeck, R. E. Lopez, L. J. Zanetti, and T. A. Potemra, Observations of solar wind pressure initiated fast mode waves at geostationary orbit and in the polar cap, *J. Atmos. Terr. Phys.*, **53**, 231, 1991.
- Huang, C. S., Evidence of periodic (2–3 hour) near-tail magnetic reconnection and plasmoid formation: Geotail observations, *Geophys. Res. Lett.*, **29**(24), 2189, doi:10.1029/2002GL016162, 2002.
- Huang, C. S., and J. C. Foster, Variations of midlatitude ionospheric plasma density in response to an interplanetary shock, *Geophys. Res. Lett.*, **28**, 4425, 2001.
- Huang, C. S., G. J. Sofko, A. V. Kustov, J. W. MacDougall, D. A. Andre, W. J. Hughes, and V. O. Papitashvili, Quasi-periodic ionospheric disturbances with a 40 min period during prolonged northward interplanetary magnetic field, *Geophys. Res. Lett.*, **27**, 1795, 2000.
- Huang, C. S., et al., Long-period magnetospheric-ionospheric perturbations during northward interplanetary magnetic field, *J. Geophys. Res.*, **106**, 13,091, 2001.
- Huang, C. S., J. C. Foster, and P. E. Erickson, Effects of solar wind variations on the midlatitude ionosphere, *J. Geophys. Res.*, **107**(A8), 1192, doi:10.1029/2001JA009025, 2002.
- Huang, C. S., J. C. Foster, L. P. Goncharenko, G. J. Sofko, J. E. Borovsky, and F. J. Rich, Midlatitude ionospheric disturbances during magnetic storms and substorms, *J. Geophys. Res.*, **108**, doi:10.1029/2002JA009608, in press, 2003a.
- Huang, C. S., G. D. Reeves, J. E. Borovsky, R. M. Skoug, Z. Y. Pu, and G. Le, Periodic magnetospheric substorms and their relationship with solar wind variations, *J. Geophys. Res.*, **108**, doi:10.1029/2002JA009704, in press, 2003b.
- Hughes, W. J., The effect of the atmosphere and ionosphere on long period magnetospheric micropulsations, *Planet. Space Sci.*, **22**, 1157, 1974.
- Hughes, W. J., Magnetospheric ULF waves: A tutorial with a historical perspective, in *Solar Wind Source of Magnetospheric Ultra-Low-Frequency Waves*, *Geophys. Monogr. Ser.*, vol. 81, edited by M. J. Engebretson, K. Takahashi, and M. Scholer, pp. 1–11, AGU, Washington, D. C., 1994.
- Kepko, L., H. E. Spence, and H. J. Singer, ULF waves in the solar wind as direct drivers of magnetospheric pulsations, *Geophys. Res. Lett.*, **29**(8), 117, doi:10.1029/2001GL014405, 2002.
- Korotova, G. I., and D. G. Sibeck, A case study of transit event motion in the magnetosphere and in the ionosphere, *J. Geophys. Res.*, **100**, 35, 1995.
- Korotova, G. I., D. G. Sibeck, T. J. Rosenberg, C. T. Russell, and E. Friis-Christensen, High-latitude ionospheric transient events in a global context, *J. Geophys. Res.*, **102**, 17,499, 1997.
- Lanzerotti, L. J., C. S. Roberts, and W. L. Brown, Temporal variations in the electron flux at synchronous altitudes, *J. Geophys. Res.*, **23**, 5893, 1967.
- Lanzerotti, L. J., C. G. MacLennan, and M. F. Robbins, Proton drift echoes in the magnetosphere, *J. Geophys. Res.*, **76**, 259, 1971.
- Lanzerotti, L. J., H. Fukunishi, A. Hasegawa, and L. Chen, Excitation of the plasmopause at ultralow frequencies, *Phys. Rev. Lett.*, **31**, 624, 1973.
- Lanzerotti, L. J., D. B. Mellen, and H. Fukunishi, Excitation of plasma density gradients in the magnetosphere at ultralow frequencies, *J. Geophys. Res.*, **80**, 3131, 1975.
- Lessard, M. R., M. K. Hudson, B. J. Anderson, R. L. Arnoldy, H. Luhr, G. D. Reeves, N. Sate, and A. T. Weatherwax, Evidence for a global disturbance with monochromatic pulsations and energetic electron bunching, *J. Geophys. Res.*, **104**, 7011, 1999.
- Lui, A. T. Y., and C. Z. Cheng, Resonance frequency of stretched magnetic field lines based on a self-consistent equilibrium magnetosphere model, *J. Geophys. Res.*, **106**, 25,793, 2001.
- Rankin, R., F. Fenrich, and V. T. Tikhonchuk, Shear Alfvén waves on stretched magnetic field lines near midnight in Earth's magnetosphere, *Geophys. Res. Lett.*, **27**, 3265, 2000.
- Reeves, G. D., T. A. Fritz, T. E. Cayton, and R. D. Belian, Multi-satellite measurements of the substorm injection region, *Geophys. Res. Lett.*, **17**, 2015, 1990.
- Reeves, G. D., R. H. W. Friedel, R. D. Belian, M. M. Meier, M. G. Henderson, T. Onsager, H. J. Singer, D. N. Baker, X. Li, and J. B. Blake, The relativistic electron response at geosynchronous orbit during the January 1997 magnetic storm, *J. Geophys. Res.*, **103**, 17,559, 1998.
- Rinnert, K., Quasi-periodic precipitation with periods between 40–60 minutes, *Ann. Geophys.*, **14**, 707, 1996.
- Samson, J. C., Three-dimensional polarization characteristics of high-latitude Pc 5 geomagnetic micropulsations, *J. Geophys. Res.*, **77**, 6145, 1972.
- Samson, J. C., J. A. Jacobs, and G. Rostoker, Latitude-dependent characteristics of long-period geomagnetic micropulsations, *J. Geophys. Res.*, **76**, 3675, 1971.
- Samson, J. C., B. G. Harrold, J. M. Ruohoniemi, R. A. Greenwald, and A. D. M. Walker, Field line resonances associated with MHD waveguides in the magnetosphere, *Geophys. Res. Lett.*, **19**, 441, 1992.
- Schulz, M., and L. J. Lanzerotti, *Particle Diffusion in the Radiation Belts*, Springer-Verlag, New York, 1974.
- Sibeck, D. G., et al., The magnetospheric response to 8-minute period strong-amplitude upstream pressure variations, *J. Geophys. Res.*, **94**, 2505, 1989.
- Thorolfsson, A., J. C. Cerisier, and M. Pinnock, Flow transients in the postnoon ionosphere: The role of solar wind dynamic pressure, *J. Geophys. Res.*, **106**, 1887, 2001.

J. C. Foster and C.-S. Huang, Haystack Observatory, Massachusetts Institute of Technology, Route 40, Westford, MA 01886, USA. (jcf@haystack.mit.edu; cshuang@haystack.mit.edu)

G. D. Reeves, Los Alamos National Laboratory, NIS-1 MS D-466, Los Alamos, NM 87545, USA. (reeves@lanl.gov)

J. H. Sastri, Indian Institute of Astrophysics, Solar Terrestrial Physics, Bangalore 560 034, India. (jhs@iiap.ernet.in)

P. Song, Center for Atmospheric Research, University of Massachusetts, Lowell, MA 01854, USA. (Paul\_Song@uml.edu)

J. Watermann, Danish Meteorological Institute, Solar-Terrestrial Physics Division, Lyngbyvej 100, DK-2100 Copenhagen O, Denmark. (jfw@dmi.dk)

K. Yumoto, Department of Earth and Planetary Sciences, Kyushu University, 6-10-1, Hakozaki, Higashi-ku, Fukuoka 812-8581, Japan. (yumoto@geo.kyushu-u.ac.jp)